ARCHIVES OF ACOUSTICS
30, 1, 57–71 (2005)

THE RESPONSE OF A HELMHOLTZ RESONATOR TO EXTERNAL EXCITATION. PART II: FLOW-INDUCED RESONANCE

M. MEISSNER

Polish Academy of Sciences
Institute of Fundamental Technological Research
Świętokrzyska 21, 00–049 Warszawa, Poland
e-mail: mmeissn@ippt.gov.pl

(*received May 24, 2004; accepted September 23, 2004*)

In the paper a phenomenon of sound production in a resonator driven by an air jet has been investigated. Measurements of sound spectra at the closed end of the resonator cavity were performed to determine the influence of the jet velocity on the frequency and amplitude of excited acoustic oscillations. It was found that in the sound generation process two ranges of the jet velocity could be distinguished where different variations of the oscillation frequency with the growing jet velocity were observed. After the onset of oscillation the frequency increased fast with growing jet velocity and the frequency increment was directly proportional to a value of jet velocity. At higher flow velocities an increase in the frequency was still observed, but the frequency growth was much smaller. The experiment has shown also that due to an excitation of mechanical vibrations of the resonator elements a rapid change in the oscillation frequency occurred. Finally, the experimental data were compared to calculation results to examine the accuracy of the theoretical model, in which a force driving the resonator was predicted from the vortex sound theory and the resonator was modelled by an equivalent impedance circuit.

Key words: sound generation, flow-induced resonance, acoustic resonators.

1. Introduction

A flow past the orifice of a cavity resonator often induces strong acoustic oscillations. This phenomenon occurs in many engineering applications such as aircraft wheel wells [1], vehicles with open sunroofs or windows [2] and pipe systems with closed side-branches [3]. The acoustic response of the resonator to a flow excitation may consist of one or a few nearly harmonic discrete components and the frequency of the dominant component is usually close to the frequency of one of the acoustic resonant modes. The frequency of the excited oscillation changes as the flow velocity varies and a range of this change depends on flow conditions (a laminar or turbulent boundary layer) and the resonator geometry.

The phenomenon of flow-induced acoustic resonance has been investigated by many researchers. NELSON *et al.* [4, 5] studied the generation of acoustic oscillations in a Helmholtz resonator having a box cavity and a rectangular orifice. The resonance was found to be excited by periodic vortex shedding from the upstream edge of the orifice. Other researchers investigated the same phenomenon but for different resonator geometries such as: wall-mounted deep cavities (ELDER *et al.* [6], MEISSNER [7]), cavity resonators with circular neck (KHOSROPOR and MILLET [8]) and closed side-branches (BRUGGEMAN *et al.* [9], ZIADA and SHINE [10]). The details of the flow-acoustic interaction at a resonator opening have been the subject of several theoretical models. In the model of ELDER [11] the shear layer displacement was shaped by a Kelvin-Helmholtz wave, while the acoustic response of the resonant system was modelled by an equivalent impedance circuit of the resonator adopted from the organ pipe theory. A concept of the feedback mechanism was exploited in the theoretical study of MAST and PIERCE [12]. In their approach the resonator-flow system was treated as an autonomous nonlinear system and limit cycles of the system were found using the describing-function analysis. In the work of BRUGGEMAN [13] the vortex sound theory was used for the problem of flow-induced acoustic oscillations in a side-branch. In his model a force due to the convection of discrete vortices over the side-branch opening was interpreted as the acoustic source.

The present study is focused on the flow-induced acoustic oscillation in a Helmholtz resonator exposed to an air jet. The resonator geometry was the same as in Part I [14], where the system response to an acoustic excitation was examined. The variations in the frequency and amplitude of the oscillation have been studied as a function of the jet velocity (Sec. 2). To present the experimental data in a coherent form, the test results were also depicted in nondimensional form. In Sec. 3 a theoretical model was outlined to describe the flow-acoustic interaction in the resonator orifice. The theory was based on the conception of concentrated vorticity distribution in the resonator orifice. Finally, the theoretical predictions were compared with the experimental data.

2. Measurements of the resonator response

2.1. Experimental setup

Measurements were performed for a resonator used in Part I in the tests of a system response to an acoustic excitation. The resonator had a square cross-section ($s = w = 5$ cm) and a length l ranging from 1 to 16 cm (Fig. 1). A sharp-edged circular orifice with the radius $a = 6$ mm was located symmetrically in relation to the lateral cavity walls. The resonator was driven by a planar air jet. The main components of the flow system were: the inlet nozzle *1* of circular cross-section, settling chamber *2*, preliminary nozzle *3*, nozzle head *4* with the outlet nozzle of width $h = 2.3$ mm and the plate *5* of thickness $d_0 = 0.5$ mm with resonator opening (Fig. 1). The measuring system was supplied with compressed air at the maximum pressure of 0.5 MPa. The air was fed through the control valve to the settling chamber *2*, and subsequently exited via the nozzle *3* and head *4*.

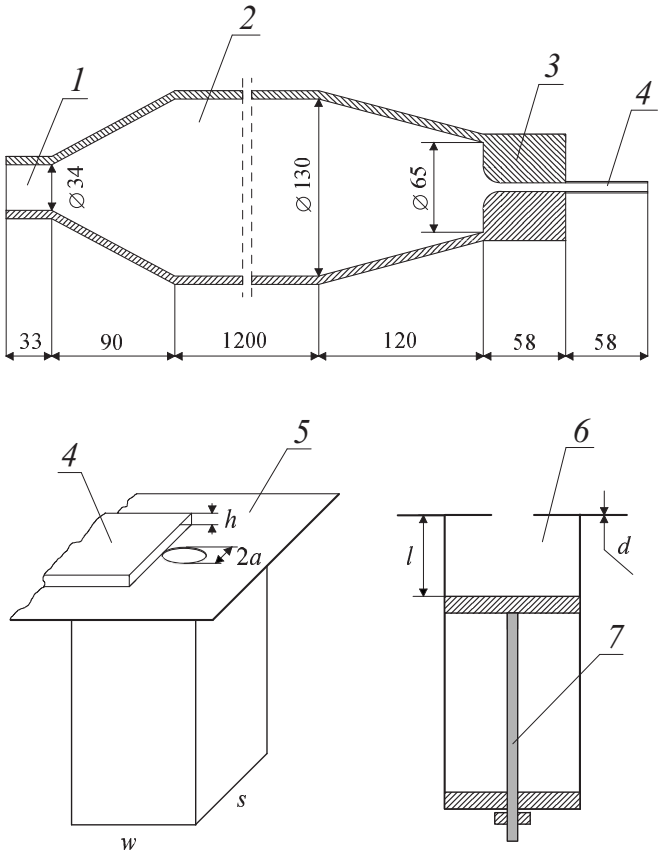

Fig. 1. Apparatus designed to produce planar air jet and resonator geometry. *1* – inlet nozzle, *2* – settling chamber, *3* – preliminary nozzle, *4* – nozzle head, *5* – orifice plate, *6* – resonator cavity, *7* – rod joining a casing of mechanical system with a piston closing the resonator cavity. Dimensions are in mm.

The volume flow, in m^3/s, was measured with the model PG 08-704 rotameter made by Prüfgerate-Werk Medingen. The average velocity U of the jet was found by dividing the volume flow by the cross-sectional area of the outlet nozzle. The acoustic pressure at the closed end of the resonator cavity was measured by a 1/4" Brüel and Kjær (B&K) microphone in conjunction with a B&K type 2618 measuring preamplifier and a B&K type 2033 spectrum analyser. The recorded sound spectra were used to determine the frequency f and the pressure amplitude p of the excited oscillation. The accuracy of the f and p measurements was 1.25 Hz and 1 Pa, respectively. To eliminate errors due to flow fluctuations, the linear averaging of sound spectra with 128 samples was used.

2.2. Tests results

Experiments were conducted for the jet velocity U between 0 and 70 m/s. The purpose of measurements was to determine the influence of the jet speed on the frequency and amplitude of the excited acoustic oscillation. In order to compare experimental data

with the results of the resonator response measurements presented in Part I, only the oscillations of frequency close to the fundamental resonant frequency of the resonator were investigated. It was found that for the smallest cavity length ($l = 1$ cm) these oscillations occurred in the range of U from 22.6 to 59.8 m/s, however for the biggest one ($l = 16$ cm) they appeared for the jet velocity between 3.8 and 12.5 m/s.

In Fig. 2 some examples of the experimental data are presented showing different variations of the oscillation frequency at low and high jet velocities. To organize the discussion, we divided the range of U into two domains: I and II, in which various relationships between f and U were observed. The lower boundary of the domain I corresponds to the lowest jet velocity at which the oscillations were observed for a given cavity length. The characteristic feature of the domain I is that the relation between f and U is independent of cavity length because data points corresponding to this domain lie in one straight line. Moreover, it was found that this relation can be described by

$$f \simeq \alpha U, \qquad \alpha = 44 \, \frac{1}{\mathrm{m}} \, , \tag{1}$$

therefore, in domain I the frequency increases directly proportionally to the jet velocity. As may be seen in Fig. 2, for each cavity length the domain I covers a very narrow range of the jet velocity. The domain II begins at the jet velocity at which the dependence between f and U becomes nonlinear. The higher boundary of this domain corresponds to the highest jet velocity at which the oscillations were still excited. A comparison of the frequency plots in Fig. 2 shows that the lower and the upper limits of domain II are different for each cavity length, but the pattern of frequency growth is very similar for all the values of l. In contrast to the domain I, in the domain II a distinctly slower increase in the oscillation frequency as a function of the jet velocity is observed.

The variations in the oscillation pressure amplitude p versus the jet velocity U for the same values of l are shown in Fig. 3. As may be seen, for all the cavity lengths the amplitude plots are similar. After the onset of oscillations, there exists a range of U were the amplitude keeps low. In the graphs it is demonstrated by a high concentration of data points. A comparison of the plots in Figs. 2 and 3 indicates that this velocity range corresponds approximately to the extent of domain I. At the jet velocities covering domain II, the pressure amplitude first grows rapidly with increasing U, next it reaches peak and finally drops down abruptly until a decay of oscillation occurs. As it results from the data in Fig. 3, a growth in the cavity length produces a distinct decrease in the maximum value of the oscillation pressure amplitude.

To correlate the experimental data obtained for different cavity lengths, we introduce three nondimensional variables. The first variable is the reduced velocity V, which is defined as the jet velocity U divided by the oscillation frequency f and the average distance $D_{\mathrm{av}} = \pi a/2$ between the upstream and downstream orifice edges [9]. The second variable is the nondimensional frequency parameter f/f_m, where f_m denotes the frequency at which the pressure amplitude for a given cavity length reaches a maximum value. The frequencies f_m are collected together with the limiting values of the f/f_m ratio for selected values of l in Table 1 and, as can be seen, the range of f/f_m variations

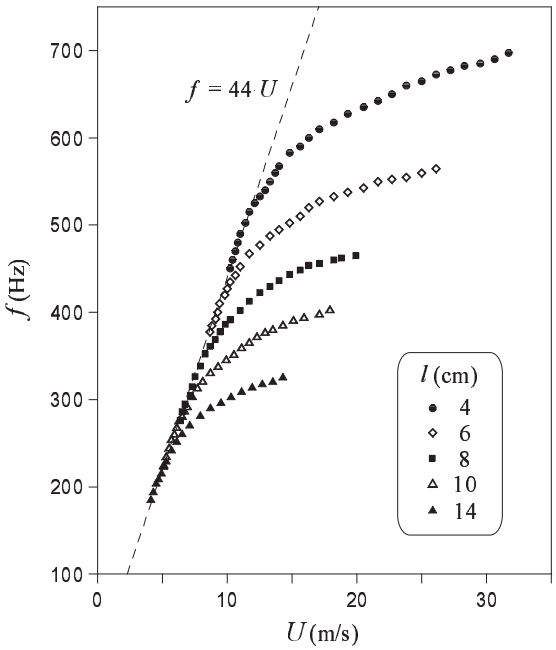

Fig. 2. Oscillation frequency versus jet velocity for resonator with cavity lengths: 4, 6, 8, 10 and 14 cm.

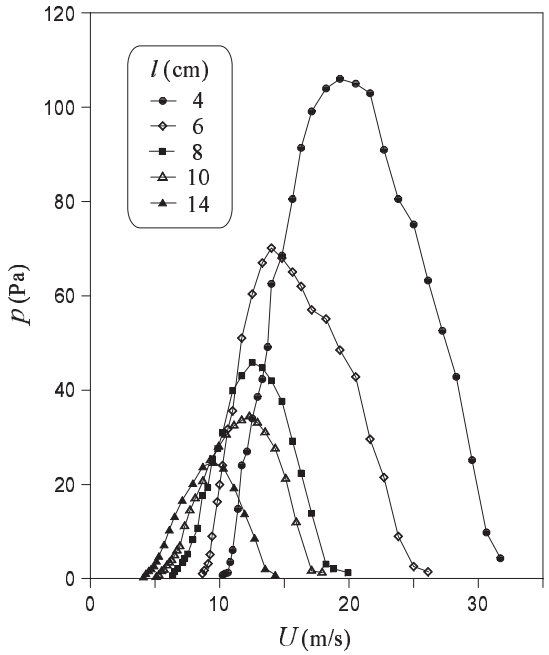

Fig. 3. Oscillation pressure amplitude versus jet velocity for resonator with cavity lengths: 4, 6, 8, 10 and 14 cm.

is similar for all the cavity lengths. In Table 1 the resonance frequencies f_0 measured in Part I are collected as well. The small difference between f_0 and f_m leads to the conclusion that a maximum resonator response occurs when the oscillation frequency is close to the resonance frequency of the system. The last variable is a relative oscillation amplitude defined as the ratio between the pressure amplitude p and the dynamic pressure $p_{\mathrm{dyn}} = \frac{1}{2}\rho U^2$, where ρ is the air density.

Table 1. Frequencies f_0 and f_m, nondimensional frequency parameter f/f_m and velocity ratio u/U for cavity length l from 4 to 16 cm.

l [cm]	f_0 [Hz]	f_m [Hz]	f/f_m	u/U
4	617.5	630.0	0.746–1.111	0.0022–0.1334
5	550.0	570.0	0.741–1.101	0.0020–0.1360
6	492.5	515.0	0.733–1.097	0.0018–0.1383
7	451.3	468.8	0.661–1.067	0.0021–0.1211
8	418.8	432.5	0.639–1.075	0.0022–0.1133
9	392.5	391.3	0.619–1.100	0.0016–0.0941
10	367.5	372.5	0.601–1.081	0.0012–0.0961
11	345.0	342.5	0.613–1.109	0.0016–0.0980
12	335.0	331.3	0.616–1.080	0.0021–0.0973
13	311.3	313.8	0.618–1.080	0.0024–0.0974
14	307.5	302.5	0.627–1.098	0.0024–0.0990
15	285.0	286.3	0.616–1.074	0.0021–0.0967
16	257.5	268.8	0.634–1.097	0.0022–0.0967

A difference between domains I and II is well observed in Fig. 4a showing the dependence of the nondimensional frequency parameter on the reduced velocity. For the frequency ratio f/f_m lower than 0.8 the data correspond to domain I. As can be seen, a characteristic feature of domain I is the nearly constant reduced velocity $(V \simeq 2.4)$. It results from the fact that in stage I the f and U are directly proportional [see Eq. (1)]. In domain II, i.e. for V above 2.4, the experimental results obtained for different cavity lengths also correlate reasonably well because data points corresponding to this domain lie approximately at the same curve. The dependence of the relative oscillation amplitude p/p_{dyn} on the reduced velocity V is presented in Fig. 4b and, as can be seen, the experimental data give also a good correlation.

In order to classify induced oscillations as regards the amplitude, we introduce, according to the work of BRUGGEMAN *et al.* [9], the velocity ratio u/U, where u is the amplitude of acoustic velocity in the resonator orifice. On the basis of this parameter three cases can be distinguished: a small-amplitude level ($u/U < 10^{-3}$), a moderate-amplitude level ($10^{-3} \leq u/U \leq 10^{-1}$) and a large-amplitude level ($u/U > 10^{-1}$).

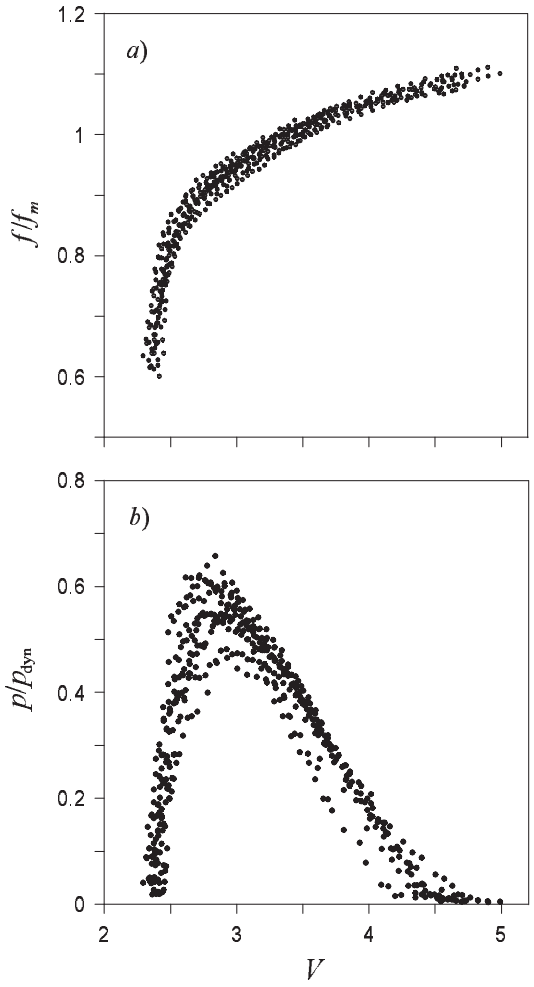

Fig. 4. (a) Nondimensional frequency parameter and (b) relative oscillation amplitude versus reduced jet velocity for resonator with cavity lengths from 4 to 16 cm.

Since it is difficult to measure the acoustic velocity directly, the values of u were computed from the pressure data using the formula for a plane wave motion in a resonator cavity

$$u = \frac{pA_c}{\rho cA} \left| \sin(kl) \right|, \tag{2}$$

which was obtained from Eq. (10) in Part I. In the above relationship c is the sound speed, $k = \omega/c$ is the wave number, $\omega = 2\pi f$, A is the orifice area and A_c is the cross-sectional area of the cavity. The limit values of the velocity ratio u/U for the considered cavity lengths are collected in Table 1. From these data it follows that in our case the oscillation amplitude can be considered as a moderate one because

the maximum value of the velocity ratio exceeds only slightly the top limit of u/U for the moderate-amplitude range.

2.3. Influence of mechanical vibrations on the resonator response

It was found in Part I that for some resonator lengths the response of the resonator to an acoustic excitation was considerably deformed by a pressure produced by mechanical vibrations. This was demonstrated by sudden drops in the cavity pressure near two frequencies. The first pressure drop was observed for the resonator length ranging from

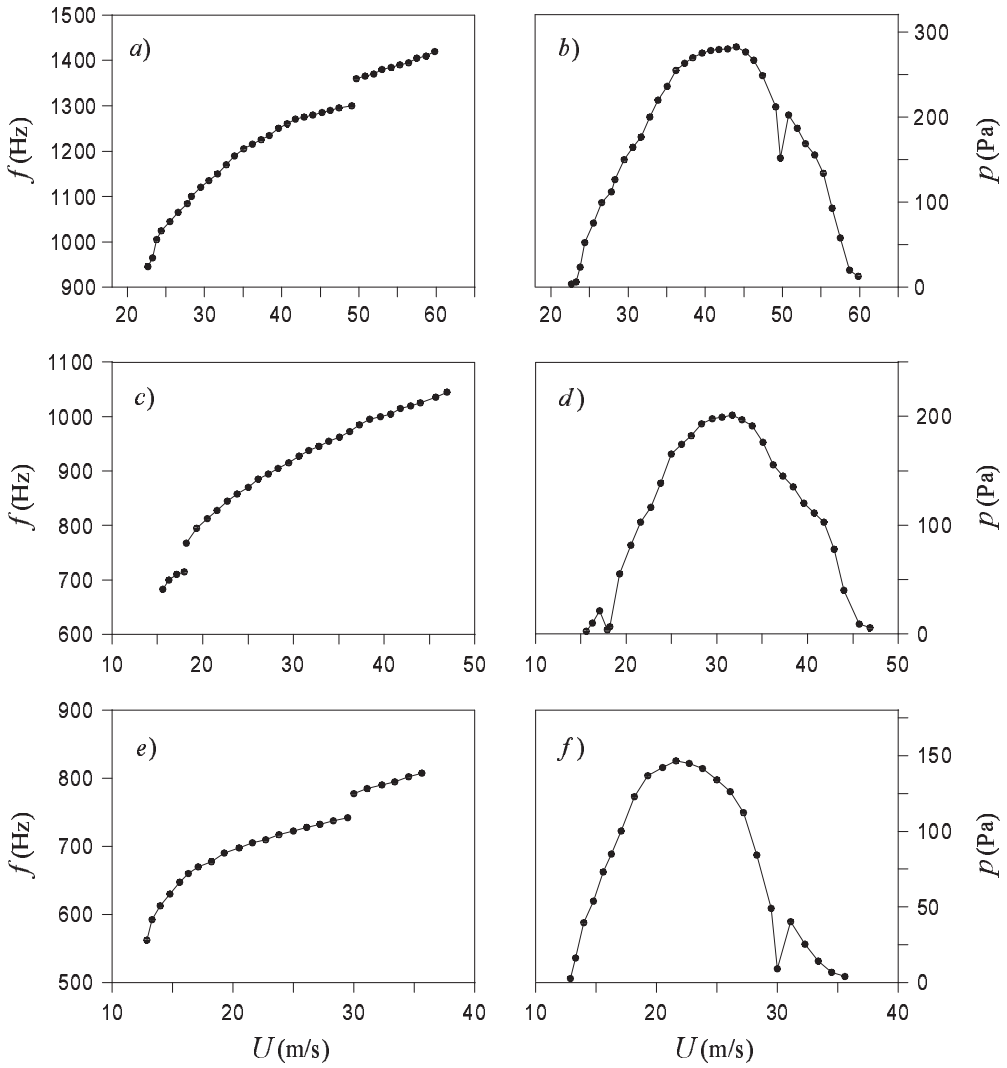

Fig. 5. Frequency and pressure amplitude of oscillation versus jet velocity for resonator with cavity lengths: (a, b) 1 cm, (c, d) 2 cm, (e, f) 3 cm.

0.8 to 1.1 cm and it appeared at a frequency close to 1320 Hz. The second pressure drop, which occurred near the frequency of 750 Hz, was detected for $l = 2-3$ cm. As was shown in Part I, the deformation of the acoustic response was caused by vibrations due to the excitation of the second and third eigenmodes of the brass rod joining the casing of the mechanical system with the piston closing the resonator cavity (Fig. 1).

The experimental results in Fig. 5 show variations in the oscillation frequency and amplitude versus the jet velocity for the cavity lengths 1, 2 and 3 cm, at which in Part I an excitation of mechanical vibrations was detected. The frequency data reveal an interesting feature of the resonator response when the sound generation is influenced by mechanical vibrations. As should be noted that the sound excitation does not occur in the neighborhood of the frequencies of mechanical vibrations. Just before the frequencies 1320 Hz (Fig. 5a) and 750 Hz (Figs. 5c,e) a sudden increase in the oscillation frequency is observed and this behavior can be attributed to a suppression of the flow-induced pressure by the pressure produced by mechanical vibrations. Measurement data depicted in Figs. 5b,d,f indicate that a jump in the oscillation frequency is accompanied by a visible decrease in the pressure amplitude.

3. Prediction of oscillation frequency and amplitude

A theoretical model describing the excitation of a resonator by an air jet was presented by the author in the work [15]. The model was based on a concept of the feedback mechanism between flow disturbances in the jet and an acoustic field in the resonator. In this approach the feedback is provided by an acoustic velocity in the resonator orifice which triggers the concentration of flow vorticity into discrete vortices when the velocity amplitude is in the moderate-amplitude range. While these vortices are convected downstream, they interact with the acoustic field in the resonator orifice and, in accordance with the vortex sound theory of HOWE [16], they produce an acoustic energy which reinforces the oscillations. The main assumptions of the theory presented in Ref. [15] are as follows:

1. A mutual interaction between the jet and the acoustic velocity leads to an asymmetric configuration of line vortices which is similar to that observed in the conventional von Kármán vortex street. Thus, the convection speed U_c of vortices is constant and can be determined from the formula

$$U_c = (U/2)\tanh(\pi h/\lambda)\,, \tag{3}$$

   where $\lambda = U_c/f$ is the distance between successive vortices in the lower and the upper line of vortices and h is a width of the jet.
2. New vortices in a lower line are initiated immediately after the moment at which the acoustic velocity is crossing the zero level and is being displaced towards the interior of the resonator cavity. The circulation Γ of the vortex increases linearly with time according to $\Gamma(t) = 0.5U^2t$.

3. The excited acoustic velocity u belongs to the moderate-amplitude range. In this case it can be assumed that the Magnus force $\mathbf{f} = \rho(\mathbf{\Omega} \times \mathbf{v})$ acting on the acoustic field is independent of u, where $\mathbf{\Omega} = \boldsymbol{\nabla} \times \mathbf{v}$ is the vorticity vector and $\mathbf{v}$ is the local fluid velocity.
4. According to the theory of HOWE [16], the force driving the resonator can be calculated from the equation $\mathbf{F} = -\int_V \mathbf{f}\, \mathrm{d}V$, where $\mathbf{F}$ is the force vector and the integral is carried out over the volume V, where the vorticity $\mathbf{\Omega}$ is non-zero.

In the theoretical model a characteristic parameter of the sound generation process is the time τ at which the vortex travels between the upstream and downstream orifice edges. For a resonator with a rectangular orifice, which was considered in Ref. [15], this time is strictly determined and is equal to D/U_c, where D is the streamwise dimension of the orifice. In the case of a resonator with a circular orifice this parameter may be determined by replacing D by the average distance $D_{\mathrm{av}} = \pi a/2$ between the upstream and downstream orifice edges. Thus, as derived in Ref. [15], the final equations for the oscillation frequency f and the acoustic velocity u can be expressed by

$$S + \tan^{-1}\left(\frac{1-\cos S}{S-\sin S}\right) = 2n\pi + \tan^{-1}(X/R)\,, \tag{4}$$

$$u = \frac{\rho U^2\left[S^2 - 2(\cos S + \sin S - 1)\right]^{1/2}}{\pi A S\left(R^2 + X^2\right)^{1/2}}\,, \tag{5}$$

where the integer n determines the hydrodynamic mode number, $S = \omega\tau = \omega D_{\mathrm{av}}/U_c$, R and X denote the resistance and the reactance of resonator, respectively and the inverse tangent function has the range $-\pi/2 < \tan^{-1}(x) < \pi/2$. According to Part I and Ref. [15], the formulae for R and X may be written as

$$R = \frac{\rho c k^2}{2\pi} + \frac{\sqrt{2\rho\mu\omega}}{A}\left(2 + \frac{d}{a}\right) + \frac{\rho u}{A}\,, \tag{6}$$

$$X = \frac{\rho c^2}{2\pi f V}\left(1 - \frac{f^2}{f_0^2}\right), \tag{7}$$

where V is the cavity volume and the resonance frequency f_0 is given as

$$f_0 \simeq \frac{c}{2\pi}\sqrt{\frac{A}{V(d+\Delta) + \frac{1}{3}Al^2}}\,, \tag{8}$$

where $\Delta = 16a(1 - 1.135\ a/s)/3\pi$ is the end correction. The first two terms in Eq. (6) describe energy losses due to the radiation of sound into the surrounding medium and the viscous action in the resonator orifice. The nonlinear term which is proportional to the velocity amplitude u appears at high amplitudes of excitation when the acoustic energy is lost on account of the vorticity generation at the resonator orifice.

To answer the question, which one of the hydrodynamic modes was excited during the experiment, one should analyze Eq. (4) in more detail. From this formula it results that the limit values of S are solutions of the following equations

$$S + \tan^{-1}\left(\frac{1-\cos S}{S-\sin S}\right) = 2n\pi \pm \pi/2, \tag{9}$$

where the signs $(-)$ and $(+)$ correspond to the lower and upper limits of S, respectively. Taking Eq. (7) into account, it is clear that the value of S is close to the upper limit when the resonator reactance X is large and this happens when the oscillation frequency f is much smaller than the resonance frequency. From Eq. (3) the expression can be derived

$$f = \frac{S\tanh(hS/2D_{\mathrm{av}})}{4\pi D_{\mathrm{av}}} \cdot U\ , \tag{10}$$

thus, when S is constant the oscillation frequency f is directly proportional to the jet velocity U. By numerical solution of Eq. (4) it was found that for the first hydrodynamic mode the upper limit of S is equal to 7.72. For such S the proportionality factor in Eq. (10) possesses the value 47.95 and this result, as seen in Fig. 2, is in agreement with the experimental data. It proves that in the considered range of the jet velocity, the first hydrodynamic mode was excited.

3.1. The numerical method

The problem of finding the frequency f and the velocity amplitude u resolves itself into a solution of Eqs. (3), (4) and (5) for a given number n of hydrodynamic mode. If we assume some initial value of the oscillation frequency f, then Eq. (3) for a specified jet velocity U can be solved numerically for U_c yielding the first approximation of S. Substitution of f and S into Eq. (5) enables to determine the velocity amplitude u. Since the resistance R includes a nonlinear term, the solution of Eq. (5) also requires a numerical procedure. Finally, we substitute the values of f, S and u into Eq. (4). If the left and right-hand sides of Eq. (4) are not equal, the initial frequency f is replaced by $f + \Delta f$, where Δf is a frequency step, and the calculations of S and u are repeated. Such a step by step procedure is performed until the numerical algorithm reaches the assumed accuracy.

3.2. Comparison between theory and experiment

By use of the numerical method outlined above, calculations of the frequency f and the velocity amplitude u were carried out for the first hydrodynamic mode and a resonator geometry used in the experiment. In order to compare experimental data with the results of the amplitude calculation, the pressure amplitude p at the closed end of the resonator cavity was computed from Eq. (2) using the velocity u and frequency f numerical data. A comparison of the frequency measurements and calculations is shown

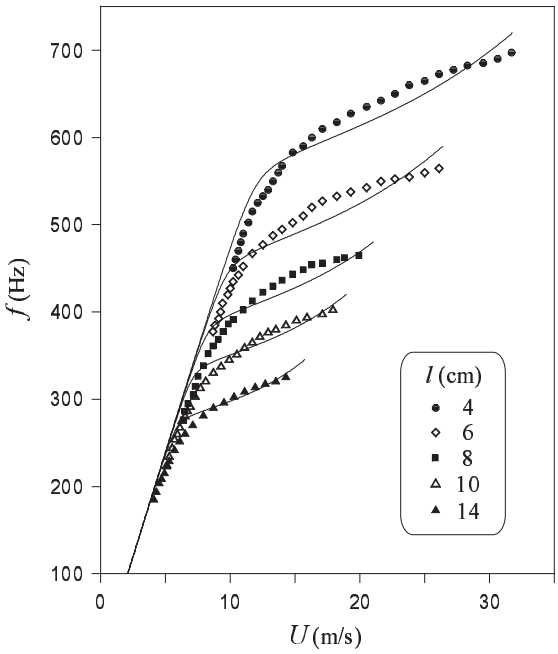

Fig. 6. Oscillation frequency versus jet velocity for resonator with cavity lengths: 4, 6, 8, 10 and 14 cm. Lines: theory.

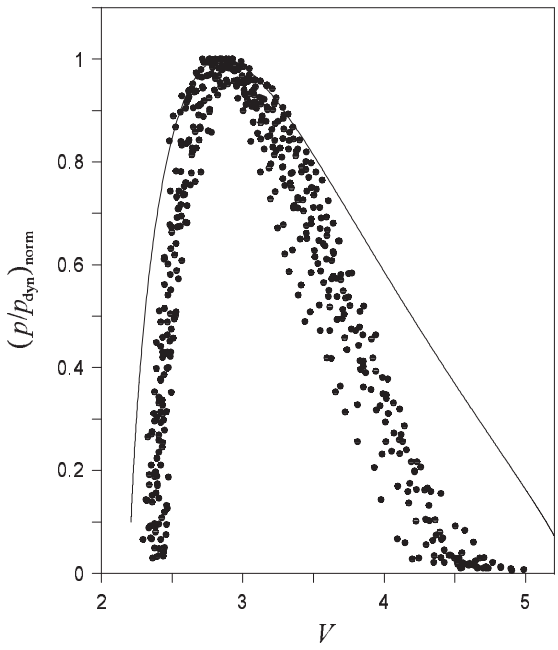

Fig. 7. Normalized relative oscillation amplitude versus reduced jet velocity. Line: theory; dots: experimental data.

in Fig. 6 and, as can be seen, the theory predicts reasonably well the influence of the jet velocity on the oscillation frequency. It results from the data in Table 2 that the theory gives fair predictions of the jet velocity U_m and the frequency f_m for a maximum pressure amplitude. However, the theory overestimates considerably this pressure, because the calculated value of p_m is 2.8–3.9 times bigger than the measured one.

Table 2. Ratios of theoretically and experimentally determined jet velocity, oscillation frequency and pressure amplitude in the case of maximum response of the resonator.

l [cm]	$\frac{(U_m)_{\rm th}}{(U_m)_{\rm exp}}$	$\frac{(f_m)_{\rm th}}{(f_m)_{\rm exp}}$	$\frac{(p_m)_{\rm th}}{(p_m)_{\rm exp}}$
4	1.171	1.011	2.794
5	1.155	0.979	2.754
6	1.184	1.003	3.208
7	1.145	0.984	3.574
8	1.168	1.005	3.497
9	1.157	1.022	3.801
10	1.100	1.002	3.599
11	1.193	1.030	3.651
12	1.113	1.012	3.732
13	1.146	1.019	3.797
14	1.119	1.010	3.786
15	1.161	1.023	3.946
16	1.224	1.047	3.845

To show the difference between the measured and predicted oscillation amplitudes in the whole range of the jet velocity, the experimental data from Fig. 4b were normalized to maximum values obtained for individual cavity lengths. The normalized experimental data together with calculation results are depicted in Fig. 7. In the latter one can see that, the theory predicts correctly a growth in the relative amplitude $p/p_{\rm dyn}$ with increasing reduced velocity V, but its accuracy is much less in the range of higher values of V where a fast decrease in $p/p_{\rm dyn}$ occurs.

4. Conclusions

An air jet flowing over a Helmholtz resonator excites acoustic oscillations with a frequency and a pressure amplitude being a function of the jet velocity. As shown by the experiment, in the case of a thin planar jet, two ranges of the jet speed U can be distinguished owing to different changes of the oscillation frequency f. In the domain I,

identified with low speed range, a rapid increase in the frequency f with growing jet velocity was observed. f and U are directly proportional and, moreover, the frequency increment was the same for all the cavity lengths. In the domain II, corresponding to higher jet speeds, a variation of the frequency was much smaller and, contrary to stage I, there was a high influence of the cavity length on the oscillation frequency (Fig. 2). In the domain II the oscillation amplitude reached a maximum value and this occurred when the oscillation frequency was close to the resonance frequency of the system (Table 1). For the smallest cavity lengths the continuous growth in the oscillation frequency with growing jet velocity was interrupted by a sudden increase in the oscillation frequency caused by an excitation of mechanical vibrations of the resonator elements (Fig. 5).

It was found that the nondimensional frequency parameter f/f_m and the relative oscillation amplitude p/p_{dyn} are the characteristic parameters of the phenomenon of flow-excited oscillations. As shown in Fig. 4, a correlation of nondimensional data is very good if one uses the reduced velocity V as the independent parameter. In accordance with the classification of BRUGGEMAN [13], the measured oscillation amplitude was recognized as moderate because the maximum value of the velocity ratio u/U only slightly exceeded the top limit of u/U for the moderate-amplitude range (Table 1).

A theoretical model [14] based on moving compact vortices and a resonance system modelled by a serial circuit with added nonlinear resistance was applied to predict a system response to flow excitation. A comparison between calculation results and the experiment data has shown a good agreement between predicted values of the oscillation frequency and the measurement data (Fig. 6). The accuracy of theory was smaller in the prediction of an absolute oscillation pressure amplitude (Table 2).

References

[1] TAM C.K., BLOCK P.J., *On the tones and pressure oscillations induced by flow over rectangular cavities*, J. Fluid Mech., **89**, 373–399 (1978).

[2] KOOK H., MONGEAU L., BROWN D.V., ZOREA S.I., *Analysis of the interior pressure oscillations induced by flow over vehicle openings*, Noise Control Eng. J., **45**, 223–234 (1997).

[3] KRIESELS P.C., PETERS M.C.A.M., HIRSCHBERG A., WIJNANDS A.P.J., IAFRATI A., RICCARDI G., PIVA R., BRUGGEMAN J.C., *High amplitude vortex-induced pulsations in a gas transport system*, J. Sound Vib., **184**, 343–368 (1995).

[4] NELSON P.A., HALLIWELL N.A., DOAK P.E., *Fluid dynamics of a flow excited resonance, part I: experiment*, J. Sound Vib., **78**, 15–38 (1981).

[5] NELSON P.A., HALLIWELL N.A., DOAK P.E., *Fluid dynamics of a flow excited resonance, part II: flow acoustic interaction*, J. Sound Vib., **91**, 375–402 (1983).

[6] ELDER S.A., FARABEE T.M., DEMETZ F.C., *Mechanisms of flow-excited cavity tones at low Mach number*, J. Acoust. Soc. Am., **72**, 532–549 (1982).

[7] MEISSNER M., *Experimental investigation of discrete sound production in deep cavity exposed to air flow*, Archives of Acoustics, **18**, 131–156 (1993).

[8] KHOSROPOUR R., MILLET P., *Excitation of a Helmholtz resonator by an air jet*, J. Acoust. Soc. Am., **88**, 1211–1221 (1990).

[9] BRUGGEMAN J.C., HIRCHBERG A., VAN DONGEN M.E.H., WIJNANDS A.P.J., GORTER J., *Self-sustained aero-acoustic pulsations in gas transport systems: experimental study of the influence of closed side branches*, J. Sound Vib., **150**, 371–393 (1991).

[10] ZIADA S., SHINE S., *Strouhal numbers of flow-excited acoustic resonance of closed side branches*, J. Fluids and Structures, **13**, 127–142 (1999).

[11] ELDER S.A., *Self-excited depth-mode resonance for a wall-mounted cavity in turbulent flows*, J. Acoust. Soc. Am., **63**, 877–890 (1978).

[12] MAST T.D., PIERCE A.D., *Describing-function theory for flow excitation of resonators*, J. Acoust. Soc. Am., **97**, 163–172 (1995).

[13] BRUGGEMAN J.C., *Flow induced pulsations in pipe systems*, Ph.D. Thesis, Eindhoven University of Technology, 1987.

[14] MEISSNER M., *The response of a Helmholtz resonator to external excitation. Part I: acoustically induced resonance*, Archives of Acoustics, **29**, 107–121 (2004).

[15] MEISSNER M., *Aerodynamically excited acoustic oscillations in cavity resonator exposed to an air jet*, Acta Acustica/Acustica, **88**, 170–180 (2002).

[16] HOWE M.S., *Contributions to the theory of aerodynamic sound with applications to excess jet noise and the theory of the flute*, J. Fluid Mech., **71**, 625–673 (1975).